PHYSICAL REVIEW B VOLUME 60, NUMBER 1 1 JULY 1999-I

Dynamic scaling of the submonolayer island size distribution during self-assembled monolayer growth

Ivo Doudevski and Daniel K. Schwartz*
Department of Chemistry, Tulane University, New Orleans, Louisiana 70118

(Received 3 December 1998; revised manuscript received 1 February 1999)

In situ atomic force microscope observations of the formation of octadecylphosphonic acid monolayers, deposited from solution onto mica, indicate that growth proceeds via the nucleation, growth, and coalescence of densely packed submonolayer islands of adsorbate molecules. Three regimes are observed: (1) an initial growth regime where nucleation of new islands is significant, (2) an aggregation regime where nucleation essentially stops and existing islands grow, and (3) a coalescence regime where individual islands merge, resulting in fewer islands. In analogy with vapor phase thin-film deposition (such as molecular-beam epitaxy) the island size distribution in the aggregation regime is predicted to show dynamic scaling behavior, indicating that at a given time, only one length scale is present. We explicitly verify this dynamic scaling assumption, showing that the island size distributions, over a range of surface coverage from 0.06–0.17, can be collapsed into a single dimensionless distribution function by the theoretically predicted scaling relationships. The shape of this distribution function implies that Ostwald ripening is not a significant factor and that the critical nucleus is ≤2 molecules. [S0163-1829(99)10725-2]

INTRODUCTION

As a flexible method of forming thin and well-defined organic coatings on a variety of solid surfaces, self-assembled monolayers (SAM's) have attracted increased attention in recent years.[1] The deposition process is attractively simple and inexpensive since the films form spontaneously upon immersion of a solid substrate into a dilute solution of organic adsorbate molecules. A number of studies, encompassing a variety of different molecule/substrate systems, indicate that the mechanism of formation involves molecular adsorption from solution, followed by aggregation into densely packed submonolayer islands on the substrate surface.[2–10] Our recent work[9] exploited the analogy with ultrahigh vacuum vapor phase thin-film growth [molecular-beam epitaxy (MBE)],[11] demonstrating that kinetic theories of two-dimensional (2D) cluster growth,[12–14] developed to explain MBE, quantitatively described the nucleation and growth kinetics of SAM islands in the early stages of film formation. Although the chemistry involved in SAM growth and MBE growth is clearly very different, the early stages of growth involve the same processes—submonolayer island nucleation and growth—and in both cases these processes are controlled by two competing rates: a deposition rate from the third dimension F and a surface diffusion rate D. In previous work[9] we studied the nucleation and growth kinetics in the early stages of growth. In the present paper, we extend the analogy with vapor phase epitaxy to include the details of the surface morphology during the later stages of growth. In particular, we explicitly demonstrate that, in the aggregation regime, the submonolayer island size distribution obeys a dynamic scaling behavior which is the signature of a wide variety of 2D aggregation processes.

The dynamic scaling assumption has been proposed to hold for a wide variety of aggregation processes, including cluster-cluster aggregation,[15] grain or bubble growth,[16] coagulation with fragmentation,[17] and a variety of droplet growth processes[18–24] ranging from metal-on-metal deposition[21] to dew formation (breath figures).[22–24] Although Monte Carlo simulations[14] have indicated the applicability of the scaling assumption to epitaxial monolayer growth, it is generally not verified experimentally because of 3D growth which becomes significant in this regime. Since the final, equilibrium state of a SAM consists of a single monolayer (there is no driving force for multilayer deposition), this system represents an ideal test for scaling theory in the later stages of monolayer growth.

The fundamental concept of the dynamic scaling assumption is that at a given stage of growth there is only a single length scale in the problem. This length can be taken to be S, the average island size, which is a function of the fractional island coverage θ. If this assumption is correct, then the island size distribution function can be written as

$$N_s(\theta)=A(S,\theta)f(s/S), \tag{1}$$

where $N_s(\theta)$ is the number density of islands containing s molecules at coverage θ. In other words, the island size distribution can be factored into two parts—one which contains all dependence on coverage and length scale, and another which is a scale-invariant fundamental distribution function.

If we integrate both sides of Eq. (1) over all island sizes s, we obtain

$$N\approx \theta/S=A(S,\theta)S\int_0^\infty du\, f(u), \tag{2}$$

where N is the total island density. This leads to the identification of $A(S,\theta)=\theta/S^2$. The general scaling form for the island size distribution predicted from the dynamic scaling assumption is therefore

$$N_s(\theta)=\theta S^{-2}f(s/S), \tag{3}$$

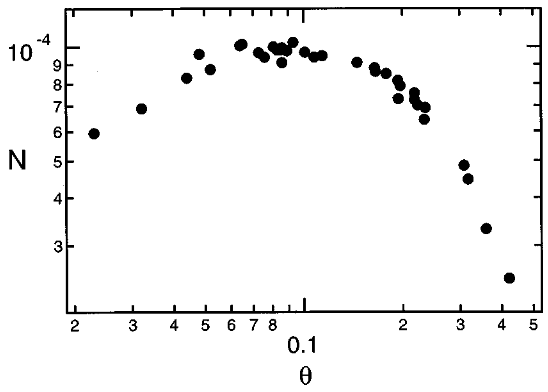

FIG. 1. A log-log plot of the number density of islands per ''site'' (estimated at 0.25 nm^2) versus fractional surface coverage showing the three regimes of growth as discussed in the text.

where the function $f(u)$ is normalized to unity. Expression (3) therefore gives a concrete prediction which can be used to verify the dynamic scaling assumption since N_s, θ, and S can all be measured directly.

EXPERIMENTAL DETAILS

Atomic force microscope (AFM) images were obtained with a Nanoscope III MMAFM (Digital Instruments, Santa Barbara, CA) in contact mode. In order to avoid surface contamination during *in situ* imaging the deposition solution came into contact with only glass, PTFE Teflon, and a fluoropolymer Kalrez o-ring (Dupont). Initially the liquid cell was filled with clean tetrahydrofuran (THF) and images were obtained of the clean mica substrate. At $t=0$, solution containing approximately 0.1 mM octadecylphosphonic acid (OPA), $CH_3(CH_2)_{17}PO(OH)_2$—dissolved in THF—was allowed to flow into the liquid cell as scanning continued over a 2×2 μm area. At various stages during monolayer growth, the scanned area was increased to 5×5 μm to check that the smaller initial scanning area contained no evidence of damage due to scanning. Image analysis was performed using NIH Image software.

RESULTS AND ANALYSIS

Figure 1 shows the total island density N as a function of fractional coverage θ extracted from AFM images 2×2 μm^2 in area. This density is normalized to a unit area of 0.25 nm^2, the approximate molecular area on the surface. Three regimes of growth are observed. For $\theta<0.06$ (growth regime) the number of islands increases, indicating that nucleation of new islands is occurring. In the range $0.06<\theta<0.17$ (aggregation regime) the island density is approximately constant. For $\theta>0.17$ (coalescence regime) the island density decreases rapidly. The AFM images in Fig. 2 trace a particular part of the growing monolayer over about 40 minutes of growth as the fractional island coverage increased from 0.06–0.16. Since these images correspond to the aggregation regime, nucleation of new islands is quite rare and coalescence of islands has not yet become a significant factor. The dominant process is the gradual growth of individual islands. The dynamic scaling approximation is expected to be appropriate for this regime.

From the full 2×2 μm^2 images we extract the fractional coverage θ and the island density distribution per molecular area. The total number of islands in each image was approximately 1600. To determine the size of submonolayer islands, it was found to be critical to account for the apparent enlarging effect due to convolution with the AFM tip. To perform an approximate deconvolution of the AFM tip size from island size we examined the apparent half width at half maximum of cross sectional profiles of the smallest observable islands in both vertical and horizontal directions for use as an upper limit. From these we established that convolution with this particular tip added approximately 7.0 nm to the radius at half maximum of an island. If one assumes a spherical tip and an island height of 2 nm, this implies a tip radius of 26 nm, which is within the typical range observed for these integral silicon nitride tips. This number was used to correct the size of islands as well as in the calculation of total coverage. This was particularly important for small islands and low coverages. The choice of the deconvolution size is the most significant uncertainty in the experiment. We discuss the effect of varying this size in the discussion section.

The island size distributions at three coverages within the aggregation regime are shown in Fig. 3(a). As one would expect qualitatively, with increasing coverage the peak position gradually moves to larger island size and the distribution broadens considerably. Figure 3(b) shows the same distribution plotted in the scaling form suggested by expression (3). The three data sets are shown to collapse onto a single function $f(s/S)=S^2\theta^{-1}N_s(\theta)$, consistent with the dynamic scaling assumption prediction. We emphasize that the quantities used to scale these data, θ and S, were measured directly, not varied in order to ''fit'' the data. The small island side of the distribution is often fit to a power law form based on empiri-

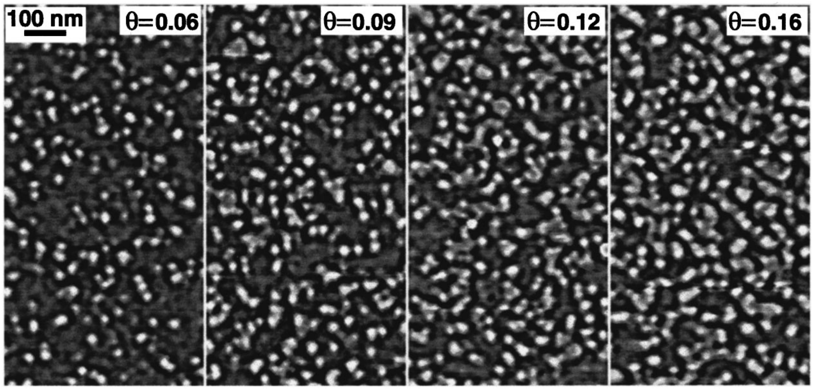

FIG. 2. Details of AFM images (500×950 nm^2) showing the same region of a monolayer during growth. The annotations on the images represent the fractional surface coverage extracted from larger 2×2 μm^2 images.

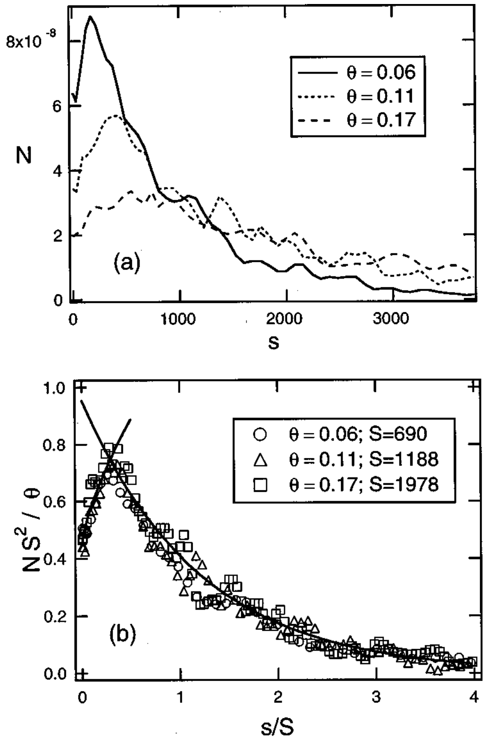

FIG. 3. Island size distributions during the aggregation regime. (a) Raw island size distributions. The number density of islands containing *s* molecules per ''site'' (estimated at 0.25 nm^2) is plotted versus *s*. The annotations reflect the fractional coverage θ for each data set. (b) The same distributions as in part (a) when scaled in a way suggested by expression (3) in the text. The inset contains the fractional coverage θ and the mean island size *S* for each data set. The fact that all three distributions collapse onto the same function is an explicit verification of the dynamic scaling assumption. The solid lines represent empirical ''fitting functions'' as discussed in the text.

cal arguments.[25,26] In this case, it is clear that the data do not extrapolate to the origin, so a simple power law dependence is not sufficient. The line drawn through the small island size data corresponds to the function $f_{\mathrm{low}}(s/S)=a_1(s/S)^i+b_1$, where $a_1=19\pm3$, $b_1=12\pm1$, and $i=0.7\pm0.1$. In a similar way, the large island side of the distribution is often observed to decay exponentially. The line draw through the large island data corresponds to the function $f_{\mathrm{high}}(s/S)=a_2\exp[-b_2(s/S)]$, where $a_2=25\pm1$ and $b_2=0.85\pm0.04$.

DISCUSSION

The fact that the island size distributions, in the aggregation regime, scale as suggested by expression (3) [as shown in Fig. 3(b)] is an explicit verification of the dynamic scaling assumption. Such morphological scaling is also observed in Monte Carlo simulations of epitaxial growth.[14] These same simulations predict power-law nucleation and growth kinetics for islands in the early growth regime which are consistent with those previously reported by us for this same SAM system.[9] The combination of short-time kinetics and later-time morphology is not trivial, i.e., the two do not necessarily follow from one another. Dynamical scaling of the island size distribution in the aggregation regime can occur in systems with various types of early growth kinetics.[21] In addition, power-law growth kinetics at early times do not necessarily imply that the island size distributions will scale as we have reported. In fact, it is generally quite difficult to explicitly verify the dynamical scaling assumption during epitaxial growth, since processes other than simple 2D island growth (such as 3D growth or dissolution/evaporation) often become significant in the aggregation regime. Taken together, therefore the consistency between simulations and experiment of both the early-time kinetics and the later-time morphology suggests that quite simple models of epitaxial growth can provide a useful description of the SAM formation process through several regimes of growth. It will also be interesting to compare the predictions of simulations for the late stages of growth (coalescence and percolation) with the actual structures observed in SAM's.

The particular shape of the scaled island size distribution is somewhat unusual. For 2D diffusion-limited cluster aggregation, the distribution function is generally observed to be fairly symmetrical about $s/S=1$ and extrapolates to the origin. A power-law behavior is observed on the low side of the peak with an exponent equal to the critical nucleus minus one, e.g., linear behavior indicates that the critical nucleus consists of two molecules.[25,26] The exception to this is when the critical nucleus is a single molecule, i.e., individual molecules can become ''stuck'' and nucleate an island. In such cases the distribution function is shown to extrapolate to a nonzero value for small island sizes and the function is monotonically decreasing. In our case, neither of these descriptions apply. There is clearly a peak in the distribution; however, it is at a value significantly less than unity and the function does not extrapolate to the origin. We hypothesize that there may be a mixture of nucleation processes occurring, some involving the collision of two molecules and others involving the spontaneous freezing of individual molecules. Our previous kinetic studies in the growth regime[9] were generally consistent with a critical nucleus of two molecules.

Clearly the details of the deconvolution of the AFM tip size from the island size manifest themselves most strongly in the small island size region of the distribution function. If one varies the choice of tip deconvolution size, the details of the island size distributions are subtly altered. For example, the exponent *i*, which is used to fit the low side of the peak to a power-law form, may range from about 0.5–0.9 for a reasonable range of deconvolution sizes. However, the basic conclusions are not altered by such a change in deconvolution size. For example, if the deconvolution size is used self-consistently to calculate island sizes and fractional coverage, the distributions are still observed to collapse onto a single function as in Fig. 3(b). In addition, this scaled function looks qualitatively the same in that it extrapolates to a nonzero value for small island sizes, is peaked at a value of s/S that is less than unity, and the peak is strongly asymmetric.

Another process one might consider in the aggregation regime is Ostwald ripening, the growth of large islands at the expense of small islands. However, there is general agreement that this process results in a distribution function that is asymmetric in the opposite way from the observed function in this case, i.e., the peak is biased towards the large island side of the distribution.[21] We therefore conclude that Ostwald ripening is not significant on the times scale we observe.

CONCLUSIONS

In situ atomic force microscopy permits a quantitative description of the surface morphology during various regimes of self-assembled monolayer growth. The data are consistent with a growth mechanism involving submonolayer island nucleation, growth, coalescence, etc. In the aggregation regime, where the number of islands is relatively constant, the island size distribution scales in a way that is consistent with the dynamic scaling assumption which has been used for a variety of aggregation processes. This morphological scaling in the aggregation regime and earlier measurements of power-law nucleation and growth kinetics at short times[9] are both consistent with Monte Carlo simulations of epitaxial growth, strengthening the link between experiment and theory over several regimes of growth. The shape of the scaled distribution function differs from those observed in simulations and is not completely understood. A qualitative analysis of this function suggests that Ostwald ripening is not significant and that the critical nucleus is $\leqslant 2$ molecules.

ACKNOWLEDGMENTS

We thank Mike Herman and Fereydoon Family for useful discussions. This work was supported by the National Science Foundation (Grant No. CHE-9614200) and the Center for Photoinduced Processes (funded by the NSF and the Louisiana Board of Regents).

---

*Author to whom correspondence should be addressed. FAX: 504-865-5596. Electronic address: dks@mailhost.tcs.tulane.edu

[1] See G. E. Poirier, Chem. Rev. **97**, 1117 (1997); and A. Ulman, *ibid.* **96**, 1533 (1996) for recent reviews.

[2] D. K. Schwartz, S. Steinberg, J. Israelachvili, and J. A. N. Zasadzinski, Phys. Rev. Lett. **69**, 3354 (1992).

[3] K. Bierbaum, M. Grunze, A. A. Baski, L. F. Chi, W. Schrepp, and H. Fuchs, Langmuir **11**, 2143 (1995).

[4] G. E. Poirier and E. D. Pylant, Science **272**, 1145 (1996).

[5] R. Yamada and K. Uosaki, Langmuir **13**, 5218 (1997).

[6] A. Eberhardt, P. Fenter, and P. Eisenberer, Surf. Sci. **397**, L285 (1998).

[7] J. T. Woodward and D. K. Schwartz, J. Am. Chem. Soc. **118**, 7861 (1996).

[8] J. T. Woodward, I. Doudevski, H. D. Sikes, and D. K. Schwartz, J. Phys. Chem. B **101**, 7535 (1997).

[9] I. Doudevski, W. A. Hayes, and D. K. Schwartz, Phys. Rev. Lett. **81**, 4927 (1998).

[10] W. A. Hayes and D. K. Schwartz, Langmuir **14**, 5913 (1998).

[11] For a recent review, see Z. Zhang and M. G. Lagally, Science **276**, 377 (1997).

[12] M. C. Bartelt and J. W. Evans, Phys. Rev. B **46**, 12 675 (1992).

[13] L.-H. Tang, J. Phys. I **3**, 935 (1993).

[14] J. G. Amar and F. Family, Phys. Rev. B **50**, 8781 (1994).

[15] T. Vicsek and F. Family, Phys. Rev. Lett. **52**, 1669 (1984).

[16] W. W. Mullins, J. Appl. Phys. **59**, 1341 (1986).

[17] F. Family, P. Meakin, and J. M. Deutch, Phys. Rev. Lett. **57**, 727 (1986).

[18] F. Family and P. Meakin, Phys. Rev. Lett. **61**, 428 (1988).

[19] F. Family and P. Meakin, Phys. Rev. A **40**, 3836 (1989).

[20] M. Zinke-Allmang, L. C. Feldman, and W. van Saarloos, Phys. Rev. Lett. **68**, 2358 (1992).

[21] M. Zinke-Allmang, L. C. Feldman, and M. H. Grabow, Surf. Sci. Rep. **16**, 377 (1992).

[22] D. Beysens and C. M. Knobler, Phys. Rev. Lett. **57**, 1433 (1986).

[23] C. M. Knobler and D. Beysens, Europhys. Lett. **6**, 707 (1988).

[24] J. L. Viovy, D. Beysens, and C. M. Knobler, Phys. Rev. A **37**, 4965 (1988).

[25] J. G. Amar and F. Family, Phys. Rev. Lett. **74**, 2066 (1995).

[26] J. G. Amar and F. Family, Thin Solid Films **272**, 208 (1996).